AD-611-225

WT-786

This document consists of 32 pages

No. 135 of 200 copies, Series A

Operation UPSHOT-KNOTHOLE

NEVADA PROVING GROUNDS

March - June 1953

Project 3.1u

SHOCK DIFFRACTION IN THE VICINITY OF A STRUCTURE(U)

Issuance Date: September 11, 1959

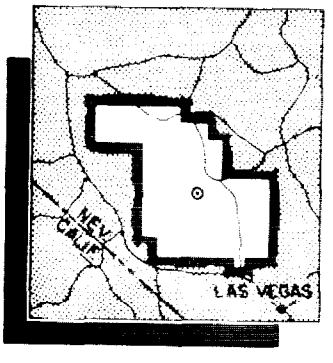

Statement C

HEADQUARTERS FIELD COMMAND, DEFENSE ATOMIC SUPPORT AGENCY
SANDIA BASE, ALBUQUERQUE, NEW MEXICO

Inquiries relative to this report may be made to

Chief, Defense Atomic Support Agency
Washington 25, D. C.

When no longer required, this document may be destroyed in accordance with applicable security regulations.

DO NOT RETURN THIS DOCUMENT

AEC Technical Information Service Extension
Oak Ridge, Tennessee

OPERATION UPSHOT-KNOTHOLE

PROJECT 3.1u

SHOCK DIFFRACTION IN THE VICINITY OF A STRUCTURE (U)

by

W. E. Morris

August 1959

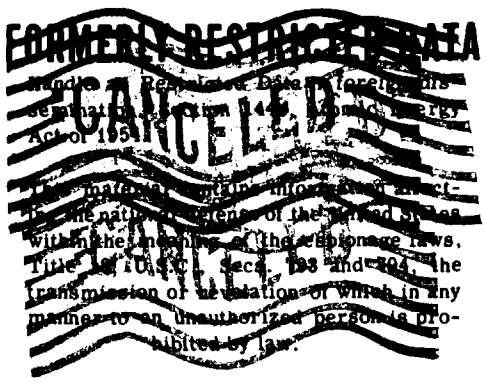

U.S. Naval Ordnance Laboratory
White Oak, Silver Spring, Maryland

ABSTRACT

A study of the shock-diffraction pattern in the vicinity of a structure was conducted to determine the loading of a structure in the vicinity of another structure and to determine at what distance the diffracted shock recovered to its free-field condition.

Fourteen Wiancko inductance-type pressure-time gages were mounted at ground level, and 5 feet above the ground, in an array to the rear and side of the 3.1t structure. This structure was 12 feet long, 6 feet wide and 6 feet high, and was located 2,200 feet from ground zero. It was oriented with its long side nearly, but not quite, parallel with the shock front. Pressure applied to the gage varied its inductance which, in turn, varied the frequency of a Hartley oscillator, of which the gage formed the inductive element. The frequency-modulated signal was transmitted by wire, and recorded on magnetic-tape recorders. In playback, the frequency-modulated signals were converted to amplitude-modulated signals and presented as pressure-time traces.

On Shot 9, the 3.1t structure was supposed to be in the regular reflection region, however. due to the presence of a heated layer near the ground, a Mach shock (a so-called thermal Mach shock) formed relatively close to ground zero, and the structure, in reality, was in a Mach region. Pressure records from all gages exhibited typical diffraction patterns in the form of initial spikes and pulses. The diffraction peaks had pressures as high as 25 percent above the undisturbed free-field peak pressure, and the diffraction effects persisted for 90 msec behind the shock front. The gages at the 5-foot height showed diffraction effects similar to, but less pronounced than, the ground-level gages. In addition, they registered the effect of a vortex that had developed on top of the structure.

On Shot 10, the 3.1t structure was also in the Mach region, but was loaded by a precursor-type pressure wave. The diffraction effect was not typical, being characterized by both pressure wave-shape distortions and a lowering of the pressure by as much as 40 percent, at times, between 50 and 300 msec after the shock-front arrival. Qualitatively, the gage records at the 5-foot height were the same as the ground-level records at corresponding locations.

Even though the shock loading on the 3.1t structure was different for Shots 9 and 10, the diffraction effects disappeared at about the same distance from the structure on both shots. Diffraction effects to both the side and rear were visible, but almost gone, at 4S, where S is a characteristic dimension of the structure (front-face height or half width, whichever is less); the effects had disappeared at 8S, and it is estimated that the blast wave again was identical with the free-field condition at 6S. Although the diffraction effect in front of the structure was not measured, it seems reasonable to expect that such an effect extended to the same distance as did the effects observed to the side and rear.

PREFACE

This is one of the reports presenting the results of the 78 projects participating in the Military Effects Tests Program of Operation Upshot-Knothole, which included eleven test detonations. For readers interested in other pertinent test information, reference is made to WT-782, "Summary Report of the Technical Director." This summary report includes the following information of possible general interest: (1) an overall description of each detonation, including yield, height of burst, ground-zero location, time of detonation, ambient atmospheric conditions at detonation, etc., for the eleven shots; (2) compilation and correlation of all project results on the basic measurements of blast and shock, thermal radiation, and nuclear radiation; (3) compilation and correlation of the various project results on weapons effects; (4) a summary of each project, including objectives and results; and (5) a complete listing of all reports covering the Military Effects Tests Program.

This project was carried out in conjunction with Projects 1.1a and 3.28.2. All three projects employed an identical integrated-instrumentation system and were conducted by the same personnel. Sincere appreciation has been acknowledged individually to project personnel for their efforts in successfully carrying out all phases of those projects (References 1 and 3). This appreciation is gratefully extended to this project.

Especial appreciation is expressed to J. Petes of the Naval Ordnance Laboratory for his assistance in the analysis of the results and review of this report.

CONTENTS

TABLES

SHOCK DIFFRACTION IN THE VICINITY OF A STRUCTURE

OBJECTIVES

The objectives of Project 3.1u were to determine the shock diffraction pattern in the vicinity of a structure and the distance necessary for a shock wave diffracted around a structure to recover and become identical with the free-field shock wave.

BACKGROUND

In a city complex, where structures are in close proximity to each other, the loading of many structures will be altered by blast shielding and shock-diffraction effects. It is important to know the true loading of these structures. Conversely, it is important to know at what distance a structure will cease exerting a shielding or diffraction effect. This latter information is needed not only for the city-complex situation, but also for determining adequate distances between structures in nuclear tests where free-field loading is desired.

Most studies of the interaction of shock waves with structures have pertained to blast loading on isolated structures. Relatively little investigation has been made of the effect of a structure on the free-field shock wave or on the shock loading of another structure close by. A limited number of laboratory shock-tube experiments, a few high-explosive field tests, and still fewer full-scale nuclear tests have been conducted on the shielding effect of one structure on the loading of another structure.[1] Again, a few shock-tube experiments have been conducted on the effects of a model structure on the incident shock wave. However, up to the time of Operation Upshot-Knothole, no field tests had been conducted.

It was this state of affairs that prompted the shock-diffraction study. The purpose of this experiment was to measure shock-pressure times at various locations in the vicinity of a structure in order to determine the shock pattern as a function of its location relative to the structure. Also, by selecting a large enough region for the measurements, the distance at which the diffracted shock recovers and becomes identical with the free-field shock wave was to be determined.

Such a method, using isolated pressure gages, was the most practical and economic way to determine both shock recovery and the shock pattern that is presented to a shielded structure. Of course, this experiment did not produce the back-and-forth reflection between the shielding and shielded structure that would take place and be of importance if closely spaced structures were employed instead of pressure gages. On the other hand, to place a number of structures at various locations relative to one another would have been expensive and would have raised problems of complicated diffraction effects between multiple close-spaced structures.

INSTRUMENTATION

The instrumentation employed for the pressure-time measurements on Project 3.1u was identical with, and a part of, the instrumentation system used on Projects 1.1a and 3.28.2. Only a

[1] Project 3.1 (Reference 1) conducted an experiment on Upshot-Knothole on parallel walls separated by various distances. The results showed that the reflected shock from the shielded wall contributed materially to the pressure buildup on the back side of the shielding wall.

brief description will be presented here. A more detailed description of the pressure gage and its characteristics, the recording and playback system, and system errors is presented in Reference 2; Reference 3 gives still more detail on the characteristics of the pressure gage; Reference 4 describes all the projects that were instrumented, along with Project 3.1u, by the Naval Ordnance Laboratory (NOL) instrumentation system.

The pressure gage was a Wiancko twisted-tube inductance gage. Pressure applied to the twisted-tube sensing element rotated an attached armature which changed the inductance of a coil. The coil comprised the inductance of the tank circuit of a Hartley oscillator used for signal generation. Thus, a forcing-pressure signal changed the frequency of the oscillator, thereby providing the means of intelligence generation. The pressure gages were located in appropriate mounts near the 3.1t structure in a pattern presented in Figures 1 and 2.

The frequency-modulated signals were transmitted by a pair of twisted, unshielded, telephone wires, buried in the ground, to the recording instrumentation housed in a van-type trailer at 7,000 feet from ground zero. Two gage-signal frequencies, one centered at 15.4 kc and the other at 10.7 kc, were diplexed on one transmission and recording channel in order to accommodate the required number of gages. The trailer recorded the signals from approximately 85 gages per shot. All recording-instrumentation controls were unmanned at shot time, and were remotely controlled.

After each shot, the magnetic tapes were recovered and played back. The magnetic variations, in the form of frequency modulations, were converted into amplitude-time variations in discriminator units and presented in graphical form on a string oscillograph. The diplexed signals were divided into their constituent parts by means of bandpass filters in each discriminator unit, so that the original gage-induced center-frequency variations were recovered as separate pressure records.

The overall frequency response of the system was such as to respond to a step-wise positive-pressure pulse in 0.2 to 0.3 msec, the gage response being the limiting factor. The overall accuracy of the system, including instrumentation and record-interpretation errors, was approximately ± 5 percent. Time resolution of the system was approximately 0.2 msec.

LAYOUT

The 3.1t structure located at 2,200 feet from intended ground zero was selected because: (1) The structure was located where it would be loaded by shock waves of representative shapes and configurations. For Shot 9, a 12-psi shock in the regular reflection region was predicted; for Shot 10, a 10-psi shock in the Mach region. (2) The structure was nondeformable, simple in shape, and of fair size. Structure 3.1t was of reinforced-concrete construction, rectangular in shape, and 12 feet long, 6 feet high, and 6 feet deep. Although a structure of larger size would have been preferred, the only structures of such size were located at 4,900 feet from ground zero, a region where the shock wave would have had less desirable characteristics for the proposed study; i.e., 8 psi and 3 psi for Shots 9 and 10, respectively, and a Mach-shock region for both shots. (3) The structure was not near any other structures that might have distorted the diffraction pattern.

Fourteen pressure-time gages were available for the project. The problem was to place this limited number of gages in such a manner as to cover the full extent and give the full detail of the diffraction pattern in the vicinity of the structure. The gage plan selected was an array of gages at ground level, and 5 feet above the ground, arranged in three lines, one directly behind the structure, one to the side of the structure, and the third line at approximately a 45-degree angle with the other two. The full layout is presented in Figure 1. Figure 2 is a photograph of the gage installation. Though it would have been desirable, no gages were placed in front of the structure, due to the limited number of available channels. The layout was identical for Shot 9 and Shot 10.

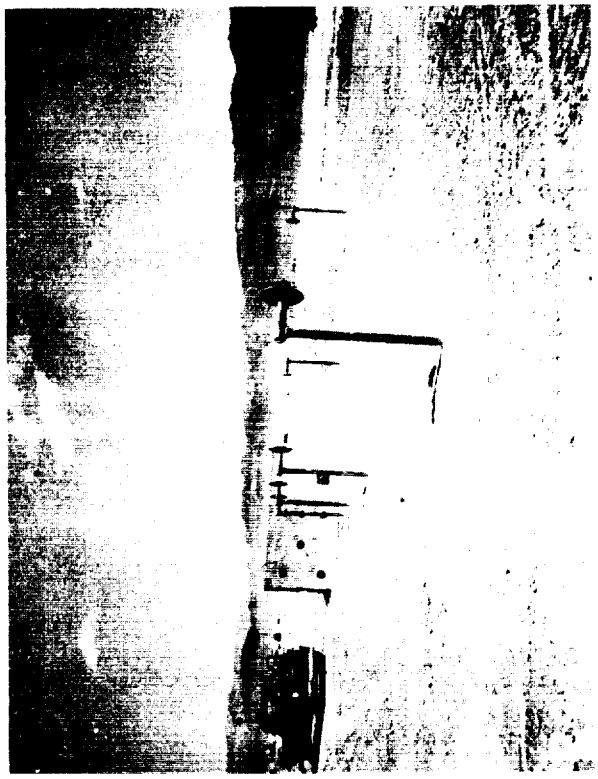

Figure 2 Photograph of the gage installation.

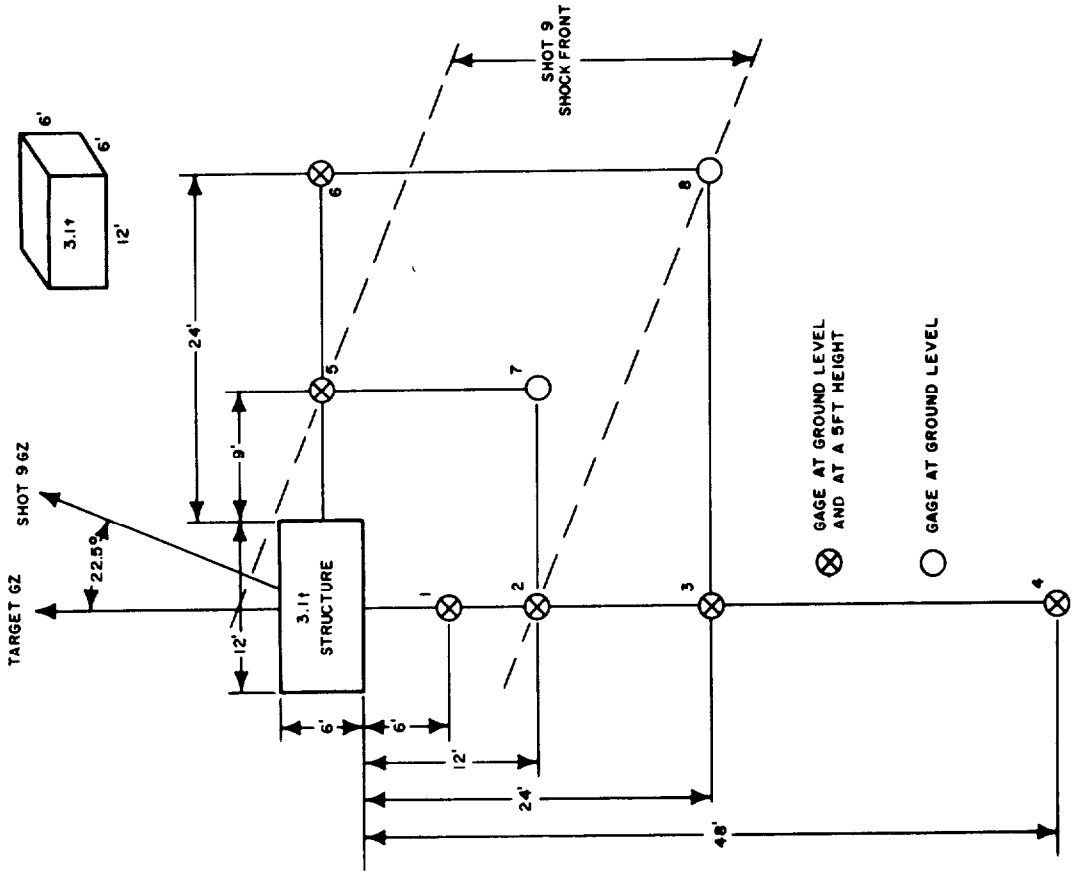

Figure 1 Gage layout.

The ground-level gages were mounted flush with the ground surface in 30-inch concrete cubes, which also provided housing for the oscillators associated with each ground level and 5-foot-high gage. The latter gages were mounted in 17-inch diameter disc-type baffles directly over the ground-level gages. The baffles were held vertically in place by means of 5-foot-high vertical poles with 18-inch horizontal extensions, as shown in Figure 2. In order best to measure shock pressures diffracted from the structure, all baffles to the side were oriented, with the gage-entry side of the baffle facing the structure. For the gages to the rear of the structure, there was no preferred baffle orientation. The front face (gage-entry side) of all vertical baffles made an angle of 5 degrees with intended ground zero, in order to ensure that the gage-entry side would be presented to the shock front in case of a moderate bombing error of ± 5 degrees.

RESULTS, SHOT 9

The yield of Shot 9 was 26.0 kt. Structure 3.1t, located nearly due west from intended ground zero, was oriented so that a long side of the structure was perpendicular to the radial line from intended ground zero in order to simplify the blast loading, i.e., the expected shock front parallel to the face of the structure. Due to bombing error, the Shot 9 burst coordinates were 837 feet south and 15 feet west of intended ground zero. As a consequence, the shock front made an angle of 22.5 degrees with the front face of the structure, as shown in Figure 1. This shock orientation must be taken into account in the analysis of the results.

For a planned burst height of 2,400 feet, the 3.1t structure, at 2,200 feet from intended ground zero, was expected to be in the regular-reflection region; the actual burst height of 2,423 feet, and a realized ground range of 2,267 feet, closely approximated this geometry. However, as it developed, the 3.1t structure was in a Mach-shock region. This occurred because of the fact that a so-called thermal-Mach shock, induced by the presence of a heated layer near the ground (from the thermal radiation from the bomb), developed at a distance much nearer ground zero than would be experienced in the absence of a heated layer. Briefly explained, a thermal Mach shock forms in a manner similar to that in which the usual Mach shock forms; i.e., as the spherical shock proceeds from ground zero, the angle that the shock front makes with the ground increases with distance, and when a critical angle is exceeded, a Mach shock forms. If a heated layer is present near the ground, the incident shock undergoes diffraction as it passes into this layer, resulting in an increase in the angle that the shock front makes with the ground. Thus, the critical angle is reached at a distance nearer ground zero than normally, and when exceeded, a thermal Mach shock is formed in the same manner as the more usual Mach shock.

While this heated layer was not hot enough to produce the better known precursor shock it was sufficient to produce an incipient-precursor condition characterized by the development of a thermal Mach shock and a rounding of the pressure peak of the shock wave. This rounding at the peak may be observed at Station F-201-0 (Figure 6), which is a free-field record near the structure. This same characteristic appears in the diffraction records, and should not be confused as a diffraction effect. For a full discussion of these thermal effects, see Reference 2. At the location of the 3.1t structure, the triple point of this thermal Mach shock was at a height of 7 feet above the ground. The evidence for this is discussed on Page 16. Thus, for the purpose of this study, the 3.1t structure and gages of Project 3.1u were all in a Mach region.

Records were obtained for all fourteen gages, and are presented in Figures 3 through 6. Gage positions relative to the structure are designated by the station numbers appearing in Figure 1 and Table 1. A second number following the station number identifies the gage height in feet. Thus, Station 2-5 indicates that the gage in question was located at Station 2 (12 feet directly behind the structure) at a height of 5 feet above the ground. Pertinent data on distance, arrival time, peak pressure, duration time, and impulse for each station is tabulated in Table 1.

Discussion of Ground Level Results. For comparison of the pressure records in the diffraction field with a pressure record in a region undisturbed by any structure, the ground-level gage along the blast line of Project 1.1a (Reference 1) nearest the 3.1u gages was used. This gage was at Station F-201, located 2,250 feet from intended ground zero (2,377 feet from true ground zero). Upon comparison, it was found to be essentially identical with the record of Station 7-0 of this study (see Figure 6, Stations 7-0 and F-201-0), and the two may be used interchangeably to represent a free field record.[2] Diffraction effects are clearly portrayed by superposition of

TABLE 1 SUMMARY OF DATA, SHOT 9

Station	Gage Height	Gage Location		Ground Range	Arrival Time	Peak Pressure	Positive Phase Duration	Positive Impulse
		To The Rear	To The Side					
	ft	ft	ft	ft	msec	psi	msec	psi-sec
1-0	0	6	0	2,275	1,692	15.1	860	3.14
1-5	5	6	0	2,275	1,692	14.2	770	3.16
2-0	0	12	0	2,281	1,693	15.2	775	2.91
2-5	5	12	0	2,281	1,693	16.0	744	3.03
3-0	0	24	0	2,292	1,701	12.5	747	3.08
3-5	5	24	0	2,292	1,701	12.7	745	3.21
4-0	0	48	0	2,314	1,712	12.5	812	3.13
4-5	5	48	0	2,314	1,712	13.3	787	3.29
5-0	0	0	9	2,262	1,684	14.0	710	2.89
5-5	5	0	9	2,262	1,685	12.6	748	2.92
6-0	0	0	24	2,256	1,680	13.0	760	2.95
6-5	5	0	24	2,256	1,681	12.0	709	2.84
7-0	0	12	9	2,275	1,691	11.8	707	2.83
8-0	0	24	24	2,281	1,695	11.8	714	2.94
F-201-0	0	On Blast Line		2,377	1,735	11.5	822	3.14
F-201-10	10	On Blast Line		2,379	1,735	13.6	763	3.17

the free-field ground-level record on all the 3.1u ground-level records, and this has been done.

In the vicinity of the structure, both to the back and to the side, the diffraction effect manifested itself as pressure spikes and pulses, near the shock front, that rose in about 5 msec to pressures 17 to 26 percent higher than the corresponding free-field pressure. Behind the structure, the pressure build-up was attributed to shock recombination after flow around-and-over the structure, and reflection from the ground directly behind the structure. To explain this reflection: after passing over the top of the structure, the vertical Mach shock front curved to a horizontal position as it traveled down the rear wall of the structure; the horizontal shock front next was reflected from the ground and traveled back up the rear wall.

These diffraction effects behind the structure were visible at Stations 1-0, 2-0, and 3-0 (Figures 3 and 4) as an initial slow pressure rise of 5 msec duration, to a spike followed by several pressure oscillations. At Station 1-0, the spike pressure was 26 percent greater than

[2] In this report, a free-field measurement is defined as a measurement under free-field conditions (as along a blast line), and, in addition, the shock being measured is in an undisturbed state. For example, a shock would be disturbed (and not a free-field shock) if it were in the diffraction field near a structure and showed diffraction effects in its pressure-time record.

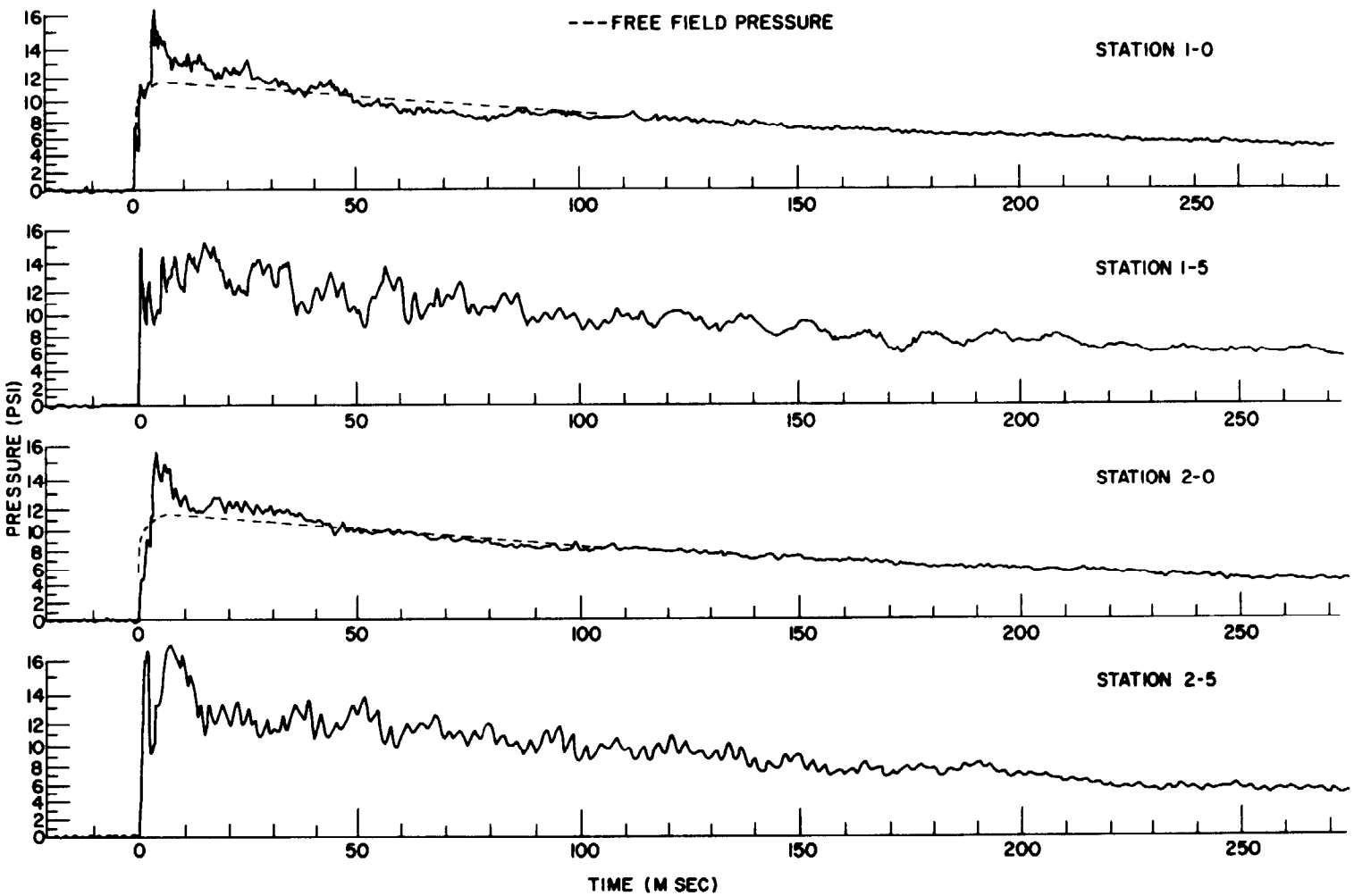

Figure 3 Shot 9, pressure-time records, Stations 1 and 2.

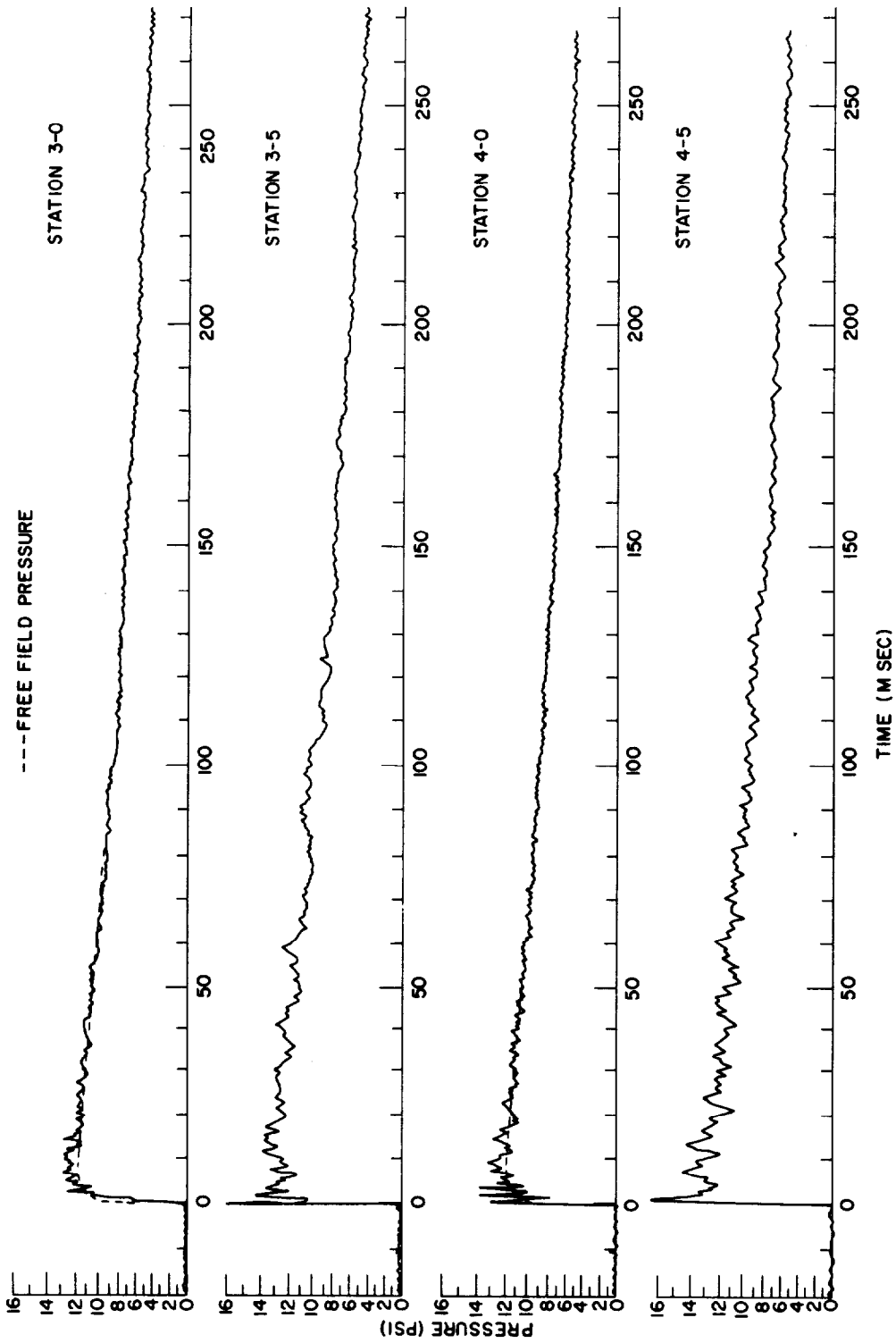

Figure 4 Shot 9, pressure-time records, Stations 3 and 4.

the free-field peak pressure. To the side of the structure, at Stations 5-0 and 6-0 (Figure 5), the undisturbed shock first arrived at the gage, and was registered as the initial pressure rise. Following this, a second pulse was observed. This second pressure pulse was clearly one that originated at the structure, for the arrival time of this pulse at each station was consistent with the time required for the shock incident on the structure to travel directly from the structure to the station. The magnitude of this diffraction pulse at Station 5-0 was 17 percent greater than the free-field peak pressure. The diffraction effects persisted for 50 msec (except for the two Stations 1-0 and 2-0 nearest the structure which showed a slight effect up to 90 msec), after which all the pressure records were identical with the free-field record.

In spatial extent, diffraction effects were observed in the records as far as 24 feet behind (Station 3-0), and 24 feet to the side (Station 6-0) of the structure. The diagonal Stations 7-0 and 8-0 were very nearly identical with the free-field record of Station F-201-0, though some slight irregularity, perhaps a vortex action or other diffraction effect, was observed at Station 8-0, and to a much less extent, at Station 7-0. At 48 feet behind the structure (Station 4-0), the shock pattern had again assumed the shape of the free-field pattern, but was 1 psi higher than the blast line value of Station F-201-0.

While this pressure difference might possibly have indicated that the diffraction effect still persisted at this distance, it almost certainly arose from difficulties associated with record interpretation, instrumentation variations, or shock irregularities not associated with any diffraction phenomenon. This conclusion was strengthened by examination of the initial pressure rise of Stations 5-0 and 6-0, shown in Figure 5. This initial pressure rise, which was also about 1 psi greater than the free-field pressure of Station F-201-0, represented the free-field peak pressure at that location, since the reflection effect from the structure did not arrive until after the free-field shock-pressure peak had been recorded.

Summarizing, diffraction effects were observed behind, and to the side of, the structure for a distance of 24 feet. At 48 feet behind (and assumed to the side), the shock wave had recovered and resumed its free-field characteristics. In terms of a representative structure dimension, S, (height or half length, whichever is less), the recovery distance was greater than 4S and less than 8S. Inspection of Table 1 and the pressure records indicates recovery was nearly complete at 4S. It is interesting to note that the diffraction effect extended as far to the side of the structure as to the back.

The diffraction effect did not make any observable contribution to the positive impulse, as may be noted in Table 1; the impulse values at any of the stations where diffraction effects were observed compared favorably, within the scatter of the data, with the free-field impulse.

Comparison of the pressure records of the first two stations behind the structure (Stations 1-0 and 2-0, Figure 3), with the pressure record of Gage P24, which was located near the ground at the center of the back face of the 3.1t structure (Figure 7), revealed close similarity in the three diffraction patterns. The initial spike had much the same shape, and the pressures of all three spikes were about 15 psi. This indicates that the shock diffraction effects observed at Stations 1-0 and 2-0 and on the structure had a common origin at the structure, and from this origin they propagated without much change out to a distance of 12 feet (2S) behind the structure.

Discussion of 5-Foot Level Results. Much less reliance was placed on the results from the gages mounted in baffles at the 5-foot height than for gages at ground level. For the measurement of accurate free-field pressure, the baffle surface should have been vertical and pointing toward ground zero. In Shot 9, this was not the case. First, the shock made an angle in azimuth of 27.5 degrees with the plane of the baffle; the bombing error introduced a 22.5-degree error to the south which was added to the planned offset of 5 degrees to the north from intended ground zero, as explained on Page 10. Further, uncertainties in proper baffle orientation were unavoidably introduced by the shock-angle variation accompanying the diffraction path of the shock in the vicinity

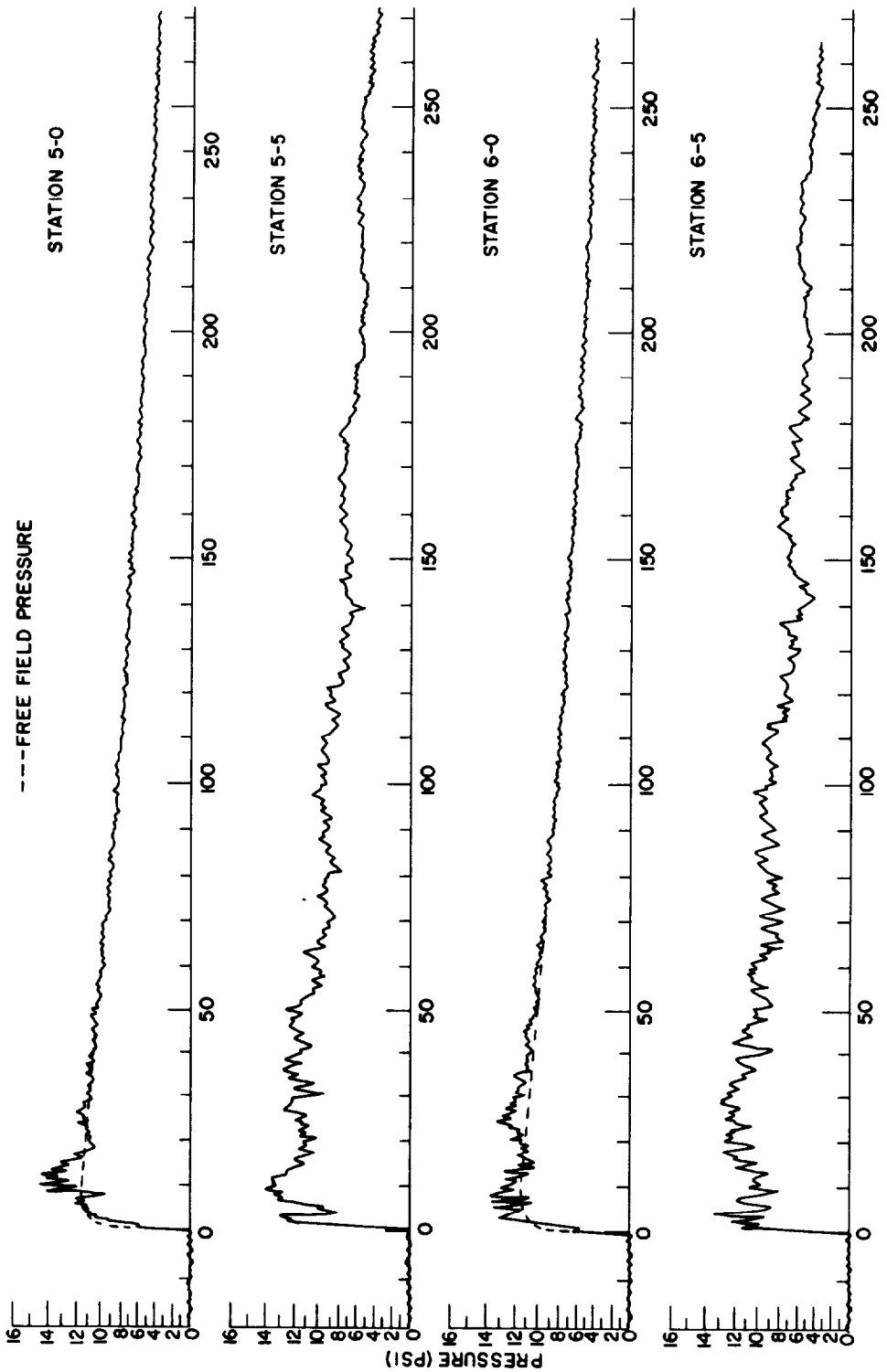

Figure 5 Shot 9, pressure-time records, Stations 5 and 6.

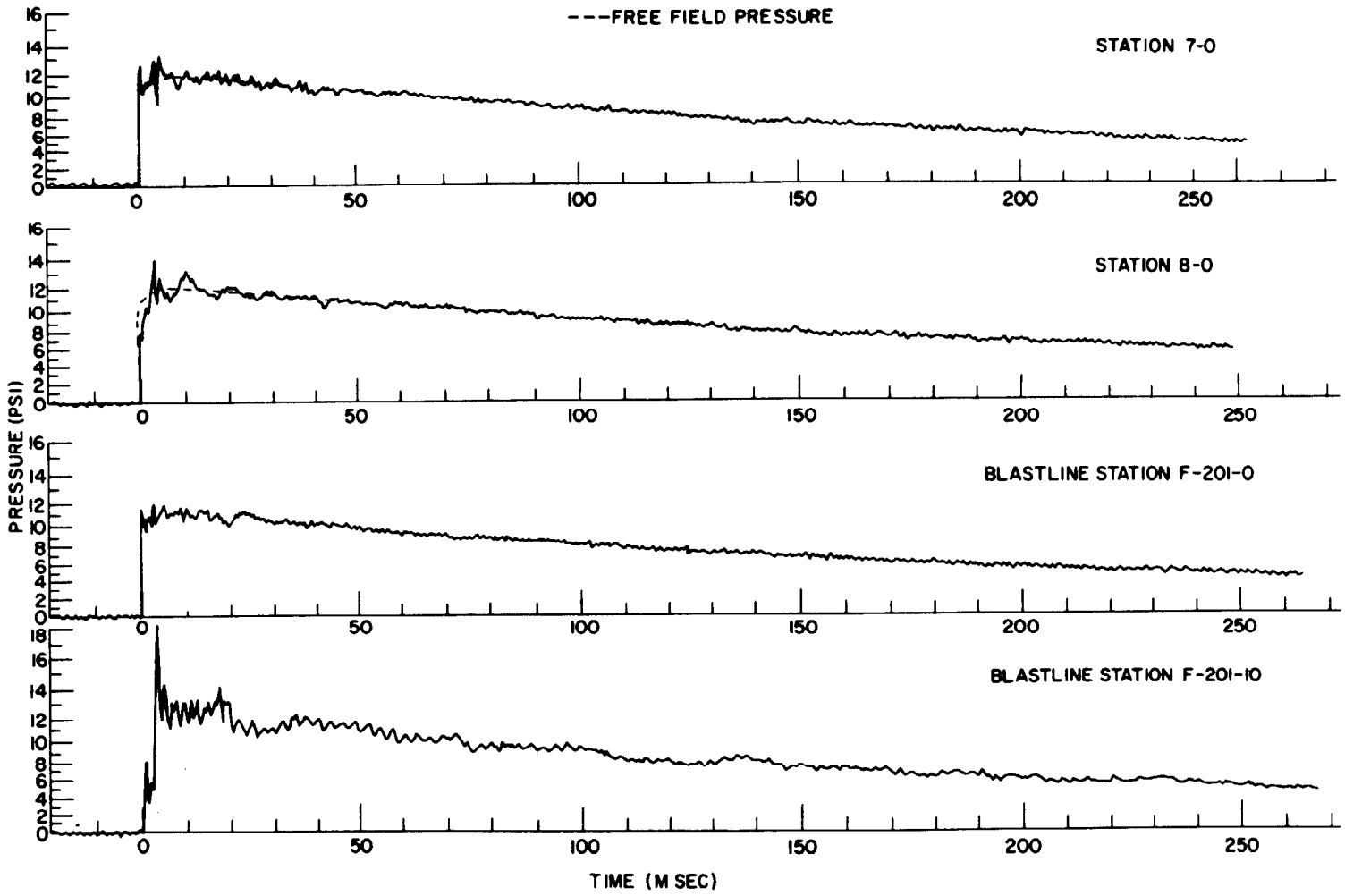

Figure 6 Shot 9, pressure-time records, Stations 7 and 8 and blast-line Station F-201.

of the structure. Still worse, the baffle placement for Stations 5-5 and 6-5 was such that the shock was incident at an angle of 27.5 degrees on the baffle side opposite the entry to the gage, and accordingly, the shock had to diffract around the baffle before registering on the gage (Figure 2).

Additional uncertainty was introduced into the 5-foot-level gage results by the whipping action of the 5-foot poles on which the gages were mounted. The gages experienced severe acceleration as a result of this whipping, which, in turn, affected the gage response, resulting in oscillations in the gage records. The oscillation is evident upon comparison of the ground level

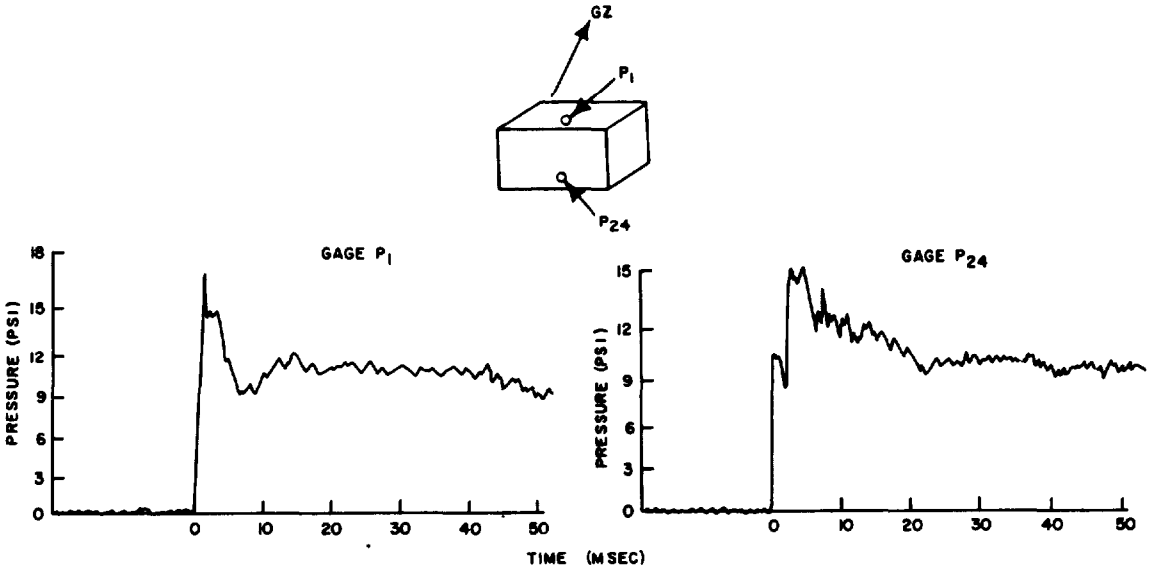

Figure 7 Shot 9, pressure-time records of Gages P1 and P24 on the 3.1t structure.

records with the 5-foot records. All in all, the 5-foot records were of value for their qualitative features, but quantitatively, they may be in error.

Superposition of a free-field record on the 5-foot-high diffraction records could not be carried out, since no free-field records were available at this height, either from Station F-201, or elsewhere.

In general, the 5-foot-level records (Figures 3, 4, and 5) indicated a diffraction spike, though not as pronounced as the ground-level spikes (at Station 1-5, 18 percent greater than the free-field-peak pressure; at Station 5-5, 4 percent). In contrast to the ground level stations, the records of 5-foot stations close to the structure (Stations 1-5, 2-5, and 5-5) dipped in pressure immediately behind the initial peak to a value 25 percent below the corresponding free-field pressure. This dip was ascribed to a vortex that developed on top of the structure, peeled off, and traveled to the nearby stations. This feature of the pressure records was similar to that in pressure records obtained from gages located on top of the 3.1t structure. For example, Figure 7 shows the record from Gage P1, which was located on the top center of the structure close to the back side. This record was quite similar to the records at Stations 1-5 and 2-5. All three records had peak-pressure values ranging from 14 to 16 psi, followed by pressure dips to values ranging between 9 to 10 psi.

The 5-foot records, in agreement with the ground-level stations, indicated that all diffraction effects were gone at 48 feet (Station 4-5) and were almost, if not completely, gone at 24 feet behind, and to the side, of the structure, (Stations 3-5 and 6-5).

of the structure. Still worse, the baffle placement for Stations 5-5 and 6-5 was such that the shock was incident at an angle of 27.5 degrees on the baffle side opposite the entry to the gage, and accordingly, the shock had to diffract around the baffle before registering on the gage (Figure 2).

Additional uncertainty was introduced into the 5-foot-level gage results by the whipping action of the 5-foot poles on which the gages were mounted. The gages experienced severe acceleration as a result of this whipping, which, in turn, affected the gage response, resulting in oscillations in the gage records. The oscillation is evident upon comparison of the ground level

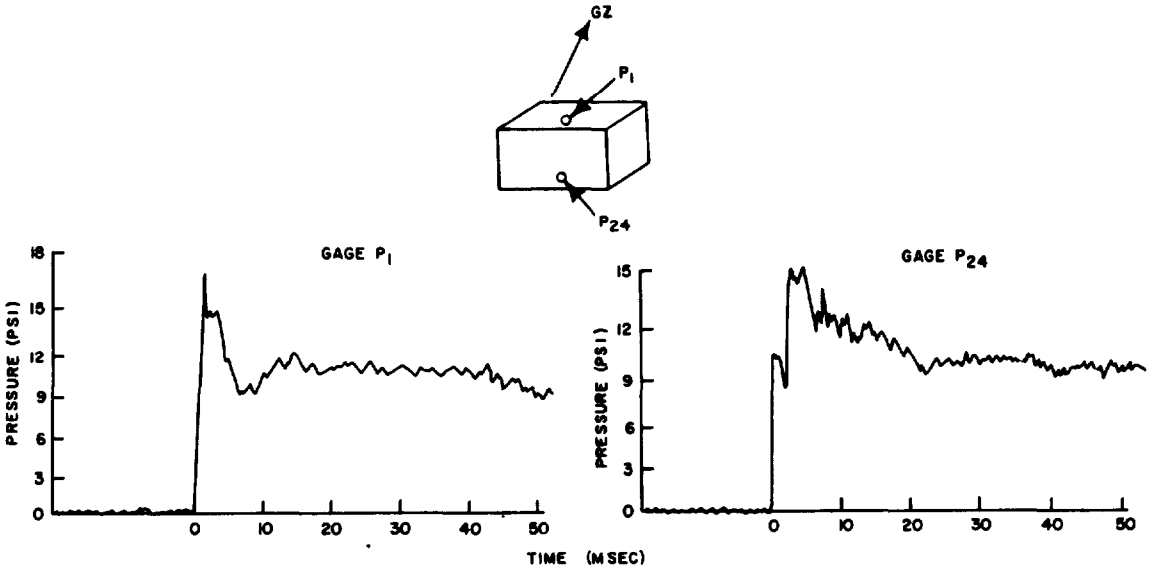

Figure 7 Shot 9, pressure-time records of Gages P1 and P24 on the 3.1t structure.

records with the 5-foot records. All in all, the 5-foot records were of value for their qualitative features, but quantitatively, they may be in error.

Superposition of a free-field record on the 5-foot-high diffraction records could not be carried out, since no free-field records were available at this height, either from Station F-201, or elsewhere.

In general, the 5-foot-level records (Figures 3, 4, and 5) indicated a diffraction spike, though not as pronounced as the ground-level spikes (at Station 1-5, 18 percent greater than the free-field-peak pressure; at Station 5-5, 4 percent). In contrast to the ground level stations, the records of 5-foot stations close to the structure (Stations 1-5, 2-5, and 5-5) dipped in pressure immediately behind the initial peak to a value 25 percent below the corresponding free-field pressure. This dip was ascribed to a vortex that developed on top of the structure, peeled off, and traveled to the nearby stations. This feature of the pressure records was similar to that in pressure records obtained from gages located on top of the 3.1t structure. For example, Figure 7 shows the record from Gage P1, which was located on the top center of the structure close to the back side. This record was quite similar to the records at Stations 1-5 and 2-5. All three records had peak-pressure values ranging from 14 to 16 psi, followed by pressure dips to values ranging between 9 to 10 psi.

The 5-foot records, in agreement with the ground-level stations, indicated that all diffraction effects were gone at 48 feet (Station 4-5) and were almost, if not completely, gone at 24 feet behind, and to the side, of the structure, (Stations 3-5 and 6-5).

the peakedness factor, i.e., the ratio of the shock dimension UT to the structure dimension H, is the same.

Without going into details of the experiments, it will suffice to summarize the results in Table 2. From the table it appears that in the SC experiments, the recovery distance, as determined by the parameters of both impulse loading and pressure on the structure, agrees well with the NOL recovery distance. The recovery distance in both cases turns out to be four in the dimensionless ratio of D (distance behind the structure) to H (height of the structure).[3] The agreement may appear surprising in view of the fact that the peakedness factors are so different. Comparison of the ARF recovery distance, as measured by the parameter of impulse loading on the structure, with the NOL recovery distance, shows a difference of about a factor of two, even though the peakedness factors are very nearly the same.

If the peakedness factor is not considered important, then the models subjected to the high-explosive type of loading scale with the nuclear test results better than the models subjected to the shock-tube type of loading. If the peakedness factor is considered to be important before scaling procedures apply, then neither the ARF nor SC experiments scale well with the nuclear test results. Perhaps equally important in the comparison is the ratio of the nuclear-test structure dimensions to the model dimensions. For the SC experiments, the ratio was 1 : 1; for ARF, the ratio was 36 : 1. Thus, comparison with the SC experiments is in reality a comparison of the effect of charge weight and not scaled structural dimensions; in contrast, comparison with ARF experiments is more nearly a comparison of the effect of scaled structural dimensions.

RESULTS, SHOT 10

The yield of Shot 10 was 14.9 kt. The burst coordinates were 137 feet south and 86 feet west of intended ground zero. This error resulted in the shock front making an angle in azimuth of 3.5 degrees with the front of the structure, instead of being parallel as planned for intended ground zero. This small error in angle can be ignored as it will have a negligible effect on the results and analysis. The burst height was 524 feet, and therefore, the 3.1t structure 2,115 feet from actual ground zero was in the Mach region.

The anticipated precursor shock formed, and the structure was in a region where a well-developed precursor shock existed. The shape of the free-field precursor shock can be observed in Figures 10 and 11. In reality, a real shock did not exist at this location; instead, there was a pressure pulse characterized by a slowly rising pressure with a broad rounded peak.

Records were obtained from eleven of the fourteen gages; those at Stations 1-5, 2-5, and 3-5 failed at zero time. The poles holding the 5-foot gages were all bent, some to the ground. Slow-speed records of all the ground-level stations are reproduced in Figures 8, 9, and 10; high-speed records of all stations are reproduced in Figures 11, 12, and 13. Data on distances, arrival

[3] The meaning of recovery distance needs to be explained. Often, recovery distance is defined as the structure-separation distance sufficient for the net-impulse loading on the shielded structure to regain its unshielded value. This usually occurs at a separation distance D considerably smaller than that obtained when the pressure record of individual pressure gage on or near the structure is used as the recovery criteria. This means that the impulse-loading parameter is a less sensitive recovery parameter than the pressure gage record. As used here, recovery is defined in terms of the more sensitive pressure parameter, and recovery is considered complete when the wave shape, pressure peak, and impulse have resumed their unshielded or free-field values.

The recovery distance of 4H quoted for the NOL recovery value in Table 2 may seem to contradict the statement of "Discussion of Ground Level Results", which states recovery occurs between 4S and 8S, which values correspond to 4H and 8H, respectively. However, if gage locations are restricted to distances directly behind the structure, and if it is recalled that the pressure record was nearly restored at 4H (peak pressure and impulse recovered but a small wave distortion then the statement is essentially correct. This is to say that recovery behind the structure takes place at a distance very close to 4H.

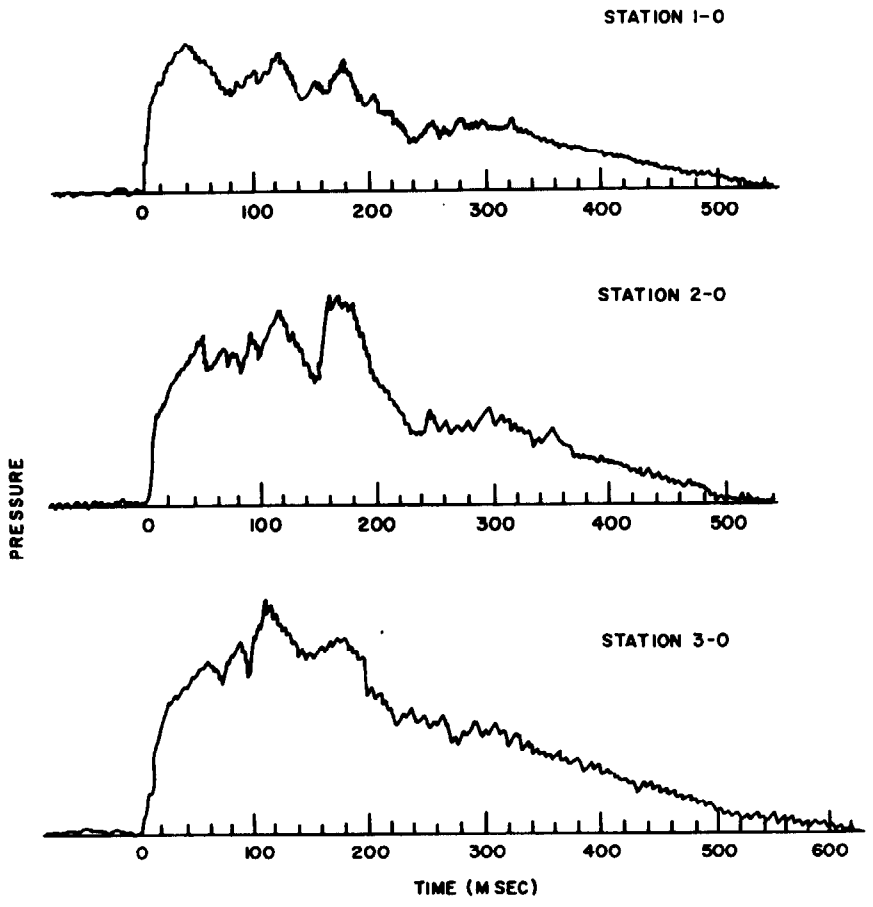

Figure 8 Shot 10, slow-speed, pressure-time records, Stations 1, 2, and 3.

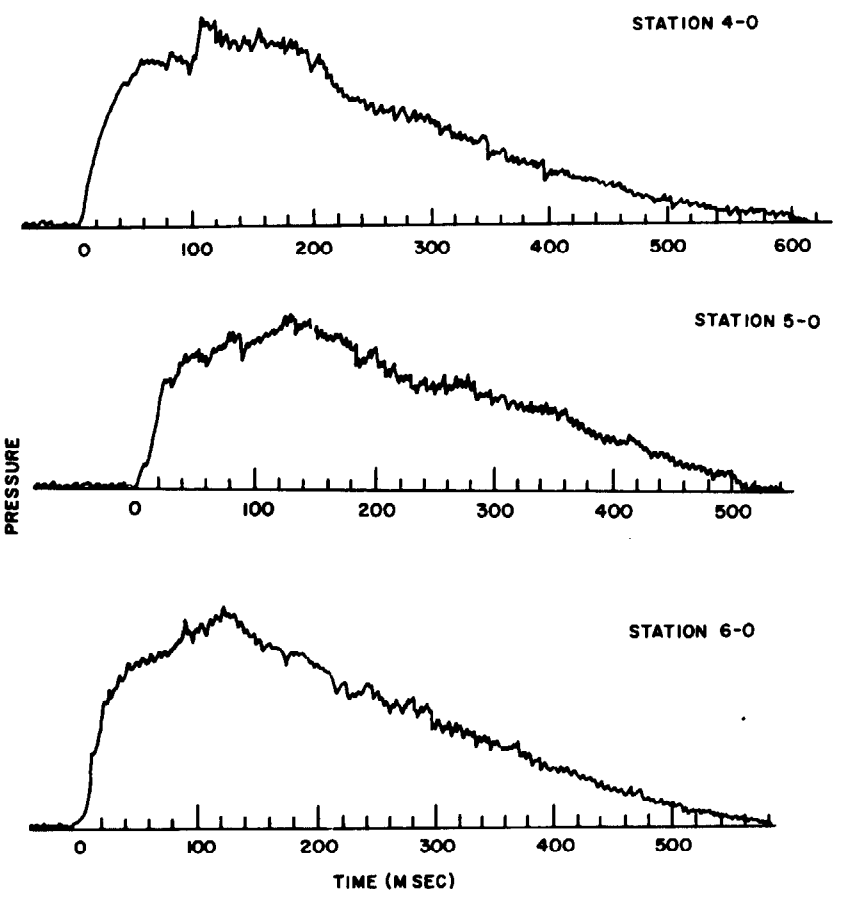

Figure 9 Shot 10, slow-speed, pressure-time records, Stations 4, 5, and 6.

times, peak pressures, durations and impulses are tabulated in Table 3. For Shot 10, the same stations and station designations were used as for Shot 9 (See Figure 1 and Table 3).

Discussion of Ground-Level Results. Slow-speed records (Figures 8 through 10) are reproduced to show best the overall shape of the precursor wave and the changes produced on it by its diffraction around the structure. The high-speed records (Figures 11 through 13 are used to measure pressure amplitudes and to reveal the fine details of the pressure wave. After de-

TABLE 3 SUMMARY OF DATA, SHOT 10

Station	Gage Height	Gage Location		Ground Range	Arrival Time	Peak Pressure	Positive Phase Duration	Positive Impulse
		To The Rear	To The Side					
	ft	ft	ft	ft	msec	psi	msec	psi-sec
1-0	0	6	0	2,115	760	6.3	520	1.59
2-0	0	12	0	2,121	760	8.5	535	2.04
3-0	0	24	0	2,133	771	9.5	610	2.56
4-0	0	48	0	2,157	784	8.2	608	2.38
4-5	5	48	0	2,157	787	8.2	620	2.66
5-0	0	0	9	2,106	747	7.0	535	2.07
5-5	5	0	9	2,106	748	7.0	525	1.92
6-0	0	0	24	2,106	749	8.5	575	2.32
6-5	5	0	24	2,106	749	8.5	—	—
7-0	0	12	9	2,121	759	8.1	555	2.15
8-0	0	24	24	2,133	770	8.2	570	2.31
F-201-0	0	On Blast Line		2,166	774	9.0	670	2.61

tailed examination of both the slow- and high-speed records as well as consideration of the pressure amplitudes, it was concluded that the records of both Stations 4-0 and 8-0 represented the free-field shock pattern at the location of the 3.1t structure better than the blast-line record of Station F-201-0 which was located laterally 200 feet away. These three records (Figures 9 and 10 were essentially identical in all respects except that the pressure record of Station F-201-0 showed a small depression that occurred in the time interval between 100 and 200 msec. It is believed that this difference, though small, is real, and represents a real change in the pressure record over this distance. For convenience, the record of Station 4-0 was selected to represent the free-field shock and was superimposed on all the other high-speed records in order to show most clearly their similarities to, and departures from, the free-field record.

The first thing to note upon examining the high-speed records is the absence of a typical diffraction effect (such as was observed on Shot 9) characterized by the presence of pressure spikes and oscillations in the first 50 msec of the pressure record. The absence of this more familiar type of diffraction effect is to be expected since there is no shock to produce transient reflections; rather, the loading is more static in nature, and the reflections that tend to develop are continuously dissipated during the time the pressure is slowly building up. The situation is analogous to the equilibrium conditions that develop after a short time in the pressure record of a true shock; i.e., the initial diffraction effect disappears and the shock pattern becomes identical with the free-field record. None of the records display any such diffraction pattern and are all, free field and those influenced by the structure, nearly alike in the initial portion of their records up to approximately 50 msec.

At times later than 50 msec, however, and extending for as long as 300 msec, the structure does affect the passing precursor wave, resulting in both lowered pressures and slow-pressure oscillations in this time interval. This may be considered as a diffraction effect different from the more familiar type and is most easily visualized in the slow-speed records of Figures 8 through 10. At Stations 1-0, 2-0, and 3-0, the pressure records show distinct dissimilarity to the superimposed free-field record of Station 4-0; the rest show slight, if any, differences. Turning now to the high-speed records of Figures 11 through 13, plus examination of peak pressures from Table 3, it is evident that the pressure records at Stations 1-0, 2-0, 3-0, and 5-0 are significantly at variance in peak pressure and/or wave shape with the superimposed free-

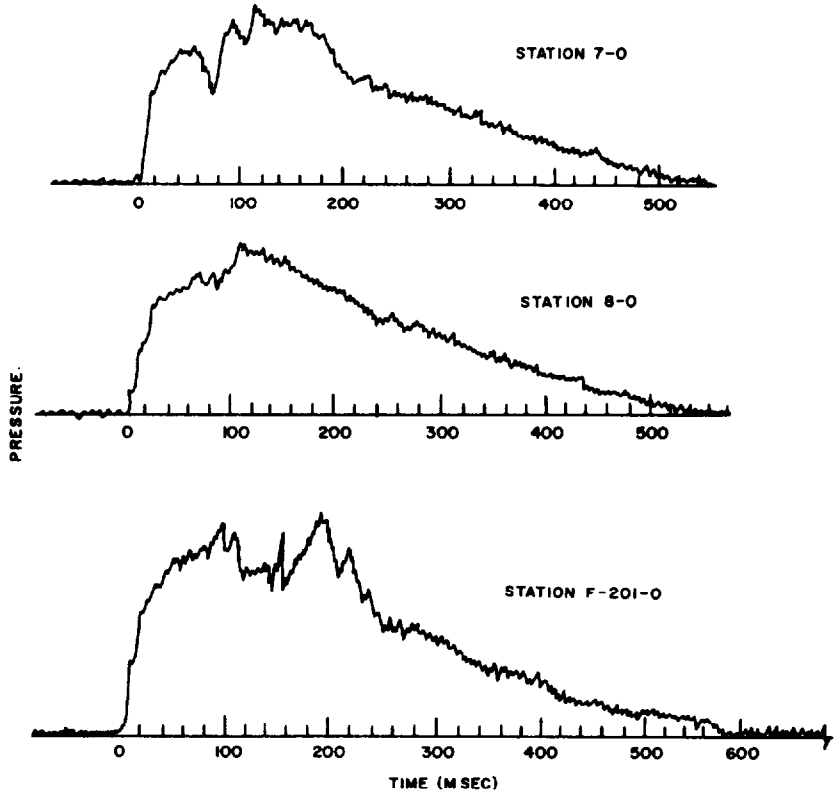

Figure 10 Shot 10, slow-speed, pressure-time records, Stations 7 and 8 and blast-line Station F-201-0.

field record. At Station 1-0 the pressure is lowered as much as 40 percent below the corresponding point on the free field record; at Station 5-0 the lowering is 25 percent.

The lower pressure and somewhat shorter time duration at Station 1-0 is definitely reflected in a resulting decreased impulse. At Stations 2-0 and 5-0, a shorter duration and decreased impulse are also indicated, but to a less degree.

Translated into distance, the pressure wave shows this new type of diffraction effect to a distance of 12 feet behind the structure, and at least 9 feet to the side; the effect has almost if not entirely disappeared at 24 feet both to the rear and to the side. In terms of dimension S (height or half length) recovery has taken place between 4S and 8S, with 4S being nearer the true recovery distance.

The Shot 10 records obtained in a precursor environment are in distinct contrast to the Shot 9 records obtained in a non-precursor region. Records from stations in the vicinity of a struc-

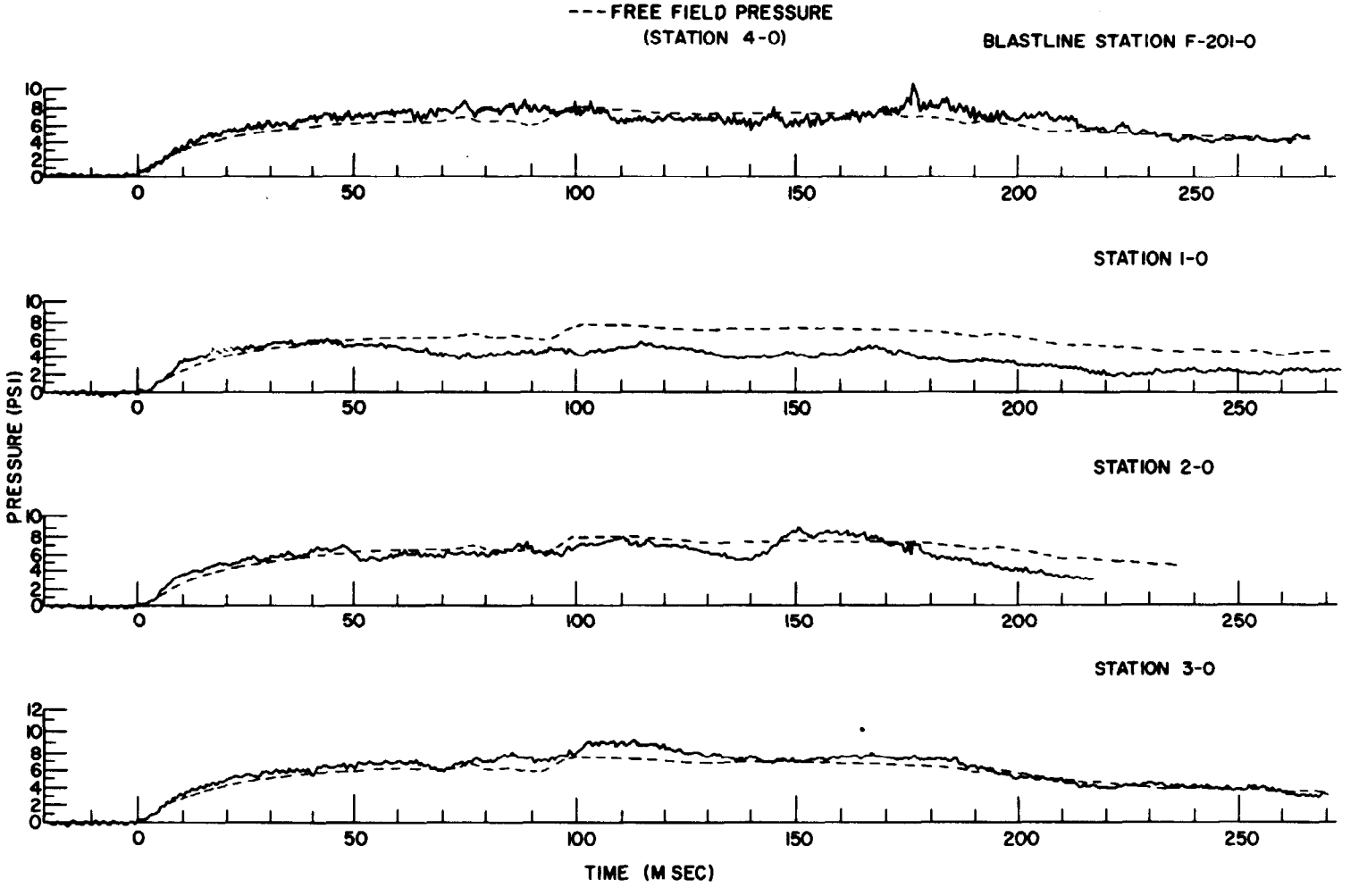

Figure 11 Shot 10, high-speed, pressure-time records, blast-line Station F-201-0 and Stations 1, 2, and 3.

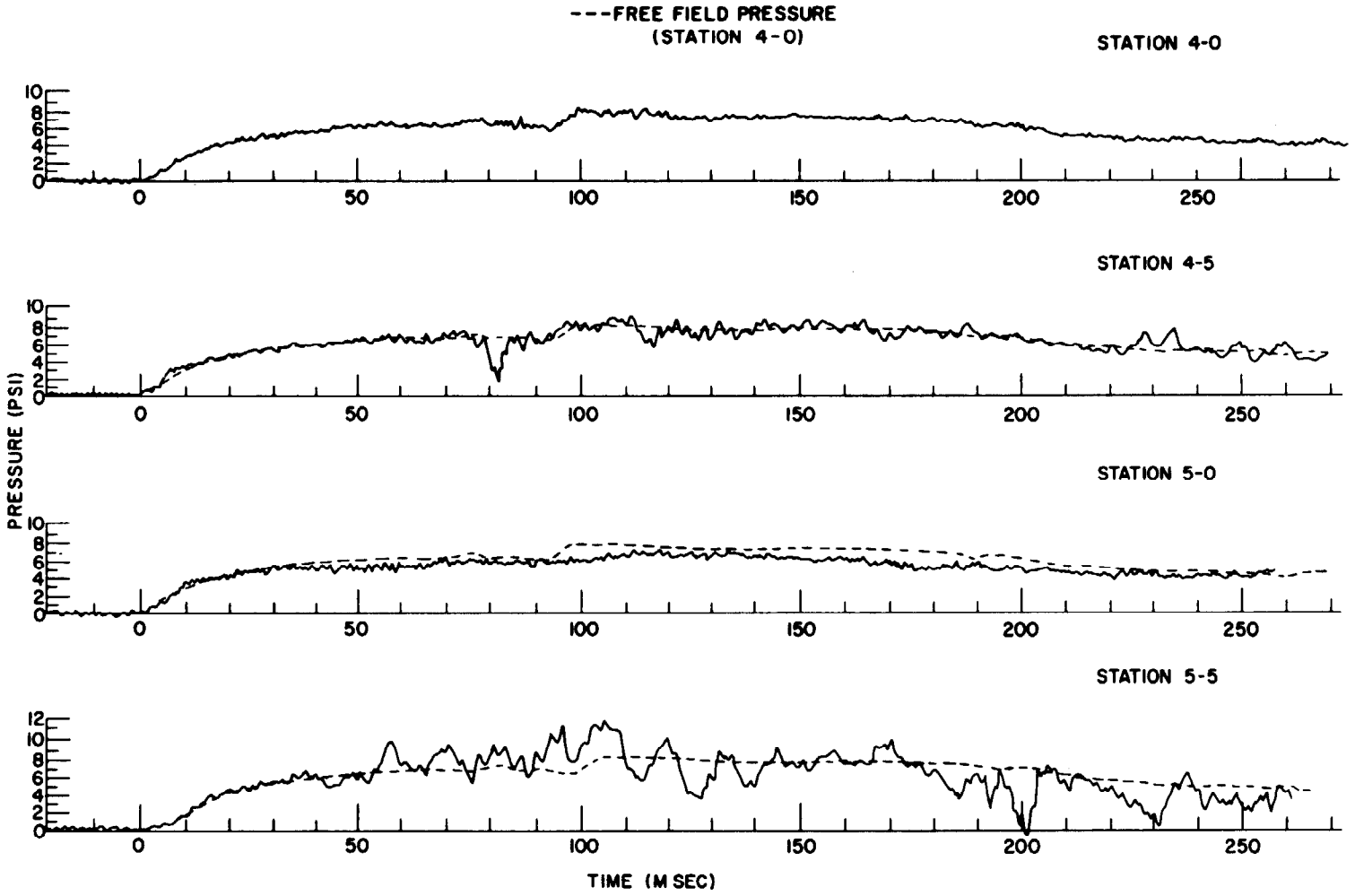

Figure 12 Shot 10, high-speed, pressure-time records, Stations 4 and 5.

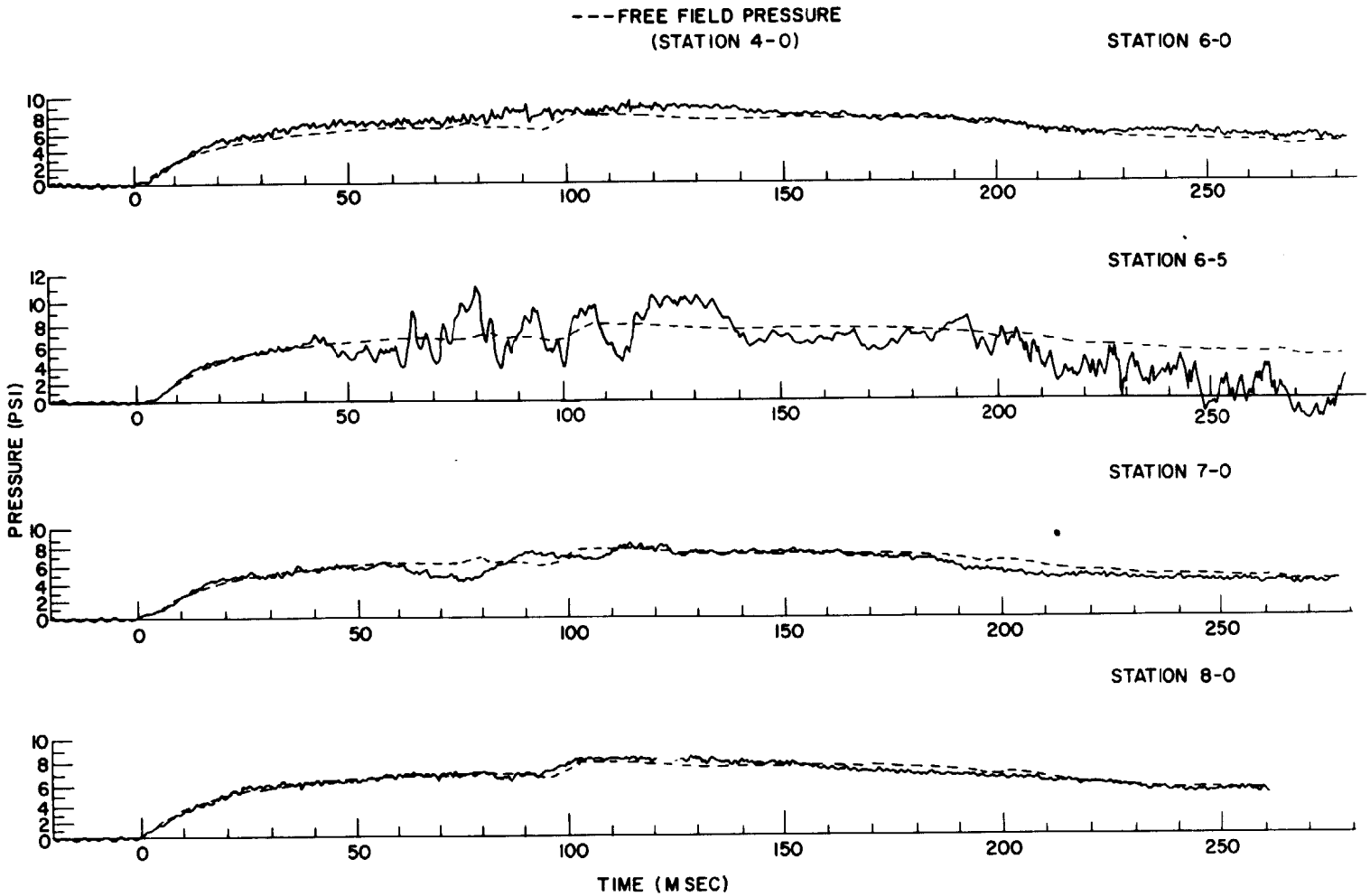

Figure 13 Shot 10, high-speed, pressure-time records, Stations 6, 7, and 8.

ture on Shot 9 exhibited diffraction patterns which lasted for only 50 msec, after which the pressure records were identical with the free-field record; corresponding records from Shot 10 showed no diffraction effects within this 50 msec time, but did show a wave-shape change and a pressure drop in the time interval from 50 to 300 msec. The diffraction effects observed on Shot 9 were to be expected; the lack of these same types of diffraction effects on Shot 10 were likewise to be expected; the diffraction effect of Shot 10 characterized by a pressure drop and wave-form variation was not expected, however, and is unexplained. As a conjecture, the pressure drop might have been due to a vortex which originated at the structure and then peeled off and traveled to the station affected.

Discussion of 5-Foot Level Results. As stated on Page 21, the three gages at Stations 1-5, 2-5, and 3-5 failed at zero time. The remaining three gages at the 5-foot height were subjected to severe acceleration effects as is evident from the fact that all the poles were badly bent. Thus, the 5-foot gage records are suspect due both to acceleration effects and orientation errors.

Comparison of the 5-foot records with the superimposed Station 4-0 record (Figure 12) indicates the results are more valid than might be expected. Excluding several oscillations caused by the effect of acceleration, the Station 4-5 record follows the Station 4-0 record remarkably well. While the records of Stations 5-5 and 6-5 have considerably more oscillation (Figures 12 and 13), nevertheless, the superimposed record passes (for the most part), through the center of the oscillations. It is, therefore, believed that the records of these two stations, under more normal acceleration conditions, would either duplicate or closely resemble the free-field records of Stations 4-0 and 4-5, as well as their respective ground-level stations. Whether the small diffraction perturbation apparent at Station 5-0 is present also at Station 5-5 cannot be ascertained because of the distortion of the record produced by the gage-acceleration effect. Further, it is believed that the peak pressure of the record at Station 4-0 represents the true peak pressure at Station 4-5, 5-5, and 6-5; i.e., the average value, which was recorded in Table 3, should be used rather than the peak value of the oscillation. Since the three stations behind the structure was lost, nothing can be inferred about diffraction effects at the 5-foot level at these locations.

DIFFRACTION EFFECTS IN FRONT OF THE STRUCTURE

As stated previously, the limited number of available channels prevented installation of gages in front of the structure. According, diffraction effects in front of the structure can only be inferred. Since diffraction effects were observed on Shot 9 out to a distance between 4S and 6S both behind and to the side of the structure, it seems reasonable to assume that these effects will be present to about the same distance in all directions. It is, therefore, postulated that diffraction effects will be present out to a distance of between 4S and 6S in front of the structure.[4] For Shot 10, where the diffraction effect was of a different nature and probably was due to a flow phenomenon rather than a reflection phenomenon, it is more difficult to surmise the extent of the diffraction effect in front of the structure. To be on the conservative side, it seems best to assume that diffraction effect would also persist out to a distance of between 4S and 6S.

CONCLUSIONS

The objectives of the experiment on diffraction effects in the vicinity of a structure were substantially met. The results were complete, of good quality, and have added new information on the subject of shock diffraction. The conclusions will: (1) provide assistance in predicating the

[4] Reference 1 reports a test situation where a wave reflected from the front face of a 6-foot high, 12-foot-wide wall was strongly evident 18 feet upstream in front of the wall.

shock loading a structure will undergo when affected by the diffraction pattern of a neighboring structure and (2) help determine the separation distance necessary for one structure to be free from the diffraction influence of another.

The conclusions pertain to three-dimensional structures; nevertheless, they apply as well to two-dimensional structures, e.g., infinitely long front face. The effects observed on three-dimensional structures will, if anything, be enhanced by two-dimensional structures; e.g., recovery distance and diffraction-peak pressure will be increased.

Common to both Shots 9 and 10, which presented radically different shock-wave patterns to the 3.1t structure, was the fact that the structure had a measurable (but dissimilar) diffraction effect on the free-field shock both to the side and to the rear of the structure for a distance of between 4S, where S is a characteristic dimension (height or half width, whichever is less). While no measurements were made, it is postulated that diffraction effects would be present at the same distance in front of the structure.

Shot 9. The shock wave incident on the 3.1t structure was a thermal Mach shock of near ideal wave form. Therefore, the structure was in a Mach region rather than in the predicted regular reflection region.

The diffraction effects produced by the shock loading around the structure were characterized as follows:

1. At ground level behind the structure an initial-pressure spike rose slowly in about 5 msec to a peak pressure which was 26 percent greater near the structure than the free-field peak pressure. This was followed by several oscillations of lesser magnitude lasting between 50 to 90 msec, after which time the pressure-time record became identical with the free-field record.
2. At the 5-foot level behind the structure the diffraction spike had a value less than the ground-level spike (but 18 percent greater than the free-field ground-level value) followed by a vortex action which reduced the pressure momentarily to a value 25 percent below the free-field value.
3. At ground level stations to the side of the structure, a pressure pulse followed the arrival of the free-field shock in a time interval consistent with the shock-travel time from the structure to the station in question, indicating this pulse had its origin at the structure. This pulse rose in 5 msec to a maximum value 17 percant greater than the free-field peak pressure. Pressure variations persisted for about 50 msec after which time the pressure-time record became identical with the free-field record.
4. At the 5-foot level to the side of the structure the pressure pulse corresponding to the ground-level diffraction pulse was reduced in magnitude (4 percent greater than the free-field value) followed by a vortex action (similar to the other 5-foot stations) which reduced the pressure momentarily to a value 25 percent below the free-field record.

In spatial extent, both behind and to the side, diffraction effects were observed at a distance of 4S and were gone at 8S. Although observable at 4S, they were not significant. So, recovery was probable at 6S; certain, at 8S.

Diffraction effects extended approximately equal distances to the rear and to the side of the structure.

Diffraction effects to a distance of 2S behind the structure were closely similar to effects observed at a position close to the ground on the rear face of the structure. Thus, the pressure pattern at appropriate positions on the structure predicted the pattern that would be observed at some distance to the rear.

The recovery distance of this full-scale diffraction experiment agreed reasonably well with scaled high-explosive experiments.

Shot 10. The shock wave incident on the 3.1t structure, which was in the Mach region was a well developed precursor wave. This was not a true shock wave, but a slowly rising pressure

pulse with a broad, rounded peak.

No typical diffraction effects, characterized by pressure spikes and pulses which develop in the first 50 msec or so behind the shock front, were observed in the vicinity of the structure.

An unusual diffraction effect was produced in the vicinity of the structure. At ground level, this effect was characterized by distortions of the free-field pressure-time curve for stations in the neighborhood of the structure along with a depression in pressure to a value 25 and 40 percent below the free-field pressure at each of the two stations nearest to the side and rear of the structure, respectively. These distortions and pressure depressions took place in the time interval from 50 to 300 msec behind the shock front. The reason for this shock perturbation or diffraction effect is not understood, but may have been due to a vortex building up on the structure and then peeling off.

The shock pattern at the 5-foot height followed the corresponding ground-level patterns, although loss of records and gage acceleration effects obscured any diffraction effects that may have been present.

Recovery of the precursor wave from the diffraction effects induced by the structure was complete not far beyond a distance of 4S from the structure, S again being the characteristic structure dimension. Behind the structure, recovery was complete between 4S and 8S. In more exact terms, recovery was nearly complete at 4S; probable at 6S; a certainty at 8S. To the side, recovery occurred between 1.5 and 4S, probably near 4S.

RECOMMENDATIONS

1. If further diffraction and shielding experiments are conducted, it is recommended that dynamic pressure measurements be included.

2. It is recommended that drag and diffraction experiments on model structures in a city complex be conducted.

REFERENCES

1. E.V. Gallagher and T.H. Shiffman; "Tests on the Loading of Building and Equipment Shapes"; Project 3.1, Operation Upshot-Knothole, WT-721, July 1955; Air Material Command, Wright-Patterson Air Force Base, Ohio; Secret Restricted Data.

2. W.E. Morris et al; "Air Blast Measurements"; Projects 1.1a and 1.2, Operation Upshot-Knothole, WT-710, August 1955; Naval Ordnance Laboratory; Secret Restricted Data.

3. J. Petes et al; "Evaluation of Wiancko and Vibration Gages and Development of New Circuitry for Atomic Blast Measurements"; Project 1.1a-1, Operation Upshot-Knothole, WT-784, February 1955; Naval Ordnance Laboratory; Official Use Only.

4. W.E. Morris and J. Petes; "Pressure Measurements for Various Projects of Program 3"; Project 3.28.2, Operation Upshot-Knothole, WT-739, December 1953; Naval Ordnance Laboratory; Confidential Restricted Data.

5. M.L. Merritt; "Shielding from Blast Waves by Parallel Structures"; AFSWP-224, October 1952; Sandia Corporation.

6. A. Ritter et al; "Shielding of Three-Dimensional Blocks"; AFSWP-989, November 1955; Armour Research Foundation; Confidential.

DISTRIBUTION

Military Distribution Categories 12 and 32

ARMY ACTIVITIES

1 Deputy Chief of Staff for Military Operations, D/A, Washington 25, D.C. ATTN: Dir. of SW&R
2 Chief of Research and Development, D/A, Washington 25, D.C. ATTN: Atomic Div.
3 Assistant Chief of Staff, Intelligence, D/A, Washington 25, D.C.
4 Chief of Engineers, D/A, Washington 25, D.C. ATTN: ENGNB
5 Chief of Engineers, D/A, Washington 25, D.C. ATTN: ENGEB
6 Chief of Engineers, D/A, Washington 25, D.C. ATTN: ENGTB
7- 8 Office, Chief of Ordnance, D/A, Washington 25, D.C. ATTN: ORDTN
9 Chief of Transportation, D/A, Office of Planning and Int., Washington 25, D.C.
10- 12 Commanding General, U.S. Continental Army Command, Ft. Monroe, Va.
13 Director of Special Weapons Development Office, Headquarters COMARC, Ft. Bliss, Tex. ATTN: Capt. Chester I. Peterson
14 President, U.S. Army Artillery Board, U.S. Continental Army Command, Ft. Sill, Okla.
15 President, U.S. Army Air Defense Board, U.S. Continental Army Command, Ft. Bliss, Tex.
16 Commandant, U.S. Army Command & General Staff College, Ft. Leavenworth, Kansas. ATTN: ARCHIVES
17 Commandant, U.S. Army Air Defense School, Ft. Bliss, Tex. ATTN: Dept. of Tactics and Combined Arms
18 Commandant, U.S. Army Armored School, Ft. Knox, Ky.
19 Commandant, U.S. Army Artillery and Missile School, Ft. Sill, Okla. ATTN: Combat Development Department
20 Commandant, U.S. Army Aviation School, Ft. Rucker, Ala.
21 Commandant, U.S. Army Infantry School, Ft. Benning, Ga. ATTN: C.D.S.
22 Commandant, U.S. Army Ordnance School, Aberdeen Proving Ground, Md.
23 Commandant, U.S. Army Ordnance and Guided Missile School, Redstone Arsenal, Ala.
24 Commanding General, Chemical Corps Training Comd., Ft. McClellan, Ala.
25 Commandant, USA Transport School, Ft. Eustis, Va. ATTN: Security and Info. Off.
26 Commanding General, The Engineer Center, Ft. Belvoir, Va. ATTN: Asst. Cmdt, Engr. School
27 Director, Armed Forces Institute of Pathology, Walter Reed Army Med. Center, 625 16th St., NW, Washington 25, D.C.
28 Commanding Officer, Army Medical Research Lab., Ft. Knox, Ky.
29 Commandant, Walter Reed Army Inst. of Res., Walter Reed Army Medical Center, Washington 25, D.C.
30- 31 Commanding General, Qm R&D Comd., QM R&D Cntr., Natick, Mass. ATTN: CBR Liaison Officer
32- 33 Commanding Officer, Chemical Warfare Lab., Army Chemical Center, Md. ATTN: Tech. Library
34 Commanding General, Engineer Research and Dev. Lab., Ft. Belvoir, Va. ATTN: Chief, Tech. Support Branch
35 Director, Waterways Experiment Station, P.O. Box 631, Vicksburg, Miss. ATTN: Library
36 Commanding Officer, Picatinny Arsenal, Dover, N.J. ATTN: ORDBB-TK
37 Commanding Officer, Diamond Ord. Fuze Labs., Washington 25, D.C. ATTN: Chief, Nuclear Vulnerability Br. (230)
38- 39 Commanding General, Aberdeen Proving Grounds, Md. ATTN: Director, Ballistics Research Laboratory
40 Commanding General, Frankford Arsenal, Bridge and Tacony St., Philadelphia, Pa.
41 Commander, Army Rocket and Guided Missile Agency, Redstone Arsenal, Ala. ATTN: Tech Library
42 Commanding General, White Sands Proving Ground, Las Cruces, N. Mex. ATTN: ORDBS-OM
43 Commander, Army Ballistic Missile Agency, Redstone Arsenal, Ala. ATTN: ORDAB-HT
44 Commanding General, Ordnance Tank Automotive Command, Detroit Arsenal, Centerline, Mich. ATTN: ORDMC-RO
45 Commanding General, Ordnance Ammunition Command, Joliet, Ill.
46 Commanding General, Ordnance Weapons Command, Rock Island, Ill.
47 Commanding General, U.S. Army Electronic Proving Ground, Ft. Huachuca, Ariz. ATTN: Tech. Library
48 Commanding General, USA Combat Surveillance Agency, 1124 N. Highland St., Arlington, Va.
49 Director, Operations Research Office, Johns Hopkins University, 6935 Arlington Rd., Bethesda 14, Md.
50 Commanding General, U.S. ORD Special Weapons - Ammunition Command, Dover, N.J.
51 Commander-in-Chief, U.S. Army Europe, APO 403, New York, N.Y. ATTN: Opot. Div., Weapons Br.

NAVY ACTIVITIES

52 Chief of Naval Operations, D/N, Washington 25, D.C. ATTN: OP-03EG
53 Chief of Naval Operations, D/N, Washington 25, D.C. ATTN: OP-36
54- 55 Chief of Naval Research, D/N, Washington 25, D.C. ATTN: Code 811
56- 57 Chief, Bureau of Aeronautics, D/N, Washington 25, D.C.
58- 62 Chief, Bureau of Aeronautics, D/N, Washington 25, D.C. ATTN: AER-AD-41/20
63 Chief, Bureau of Ordnance, D/N, Washington 25, D.C.
64 Chief, Bureau of Ships, D/N, Washington 25, D.C. ATTN: Code 423
65 Chief, Bureau of Yards and Docks, D/N, Washington 25, D.C. ATTN: D-440
66 Director, U.S. Naval Research Laboratory, Washington 25, D.C. ATTN: Mrs. Katherine H. Cass
67- 68 Commander, U.S. Naval Ordnance Laboratory, White Oak, Silver Spring 19, Md.
69 Director, Material Lab. (Code 900), New York Naval Shipyard, Brooklyn 1, N.Y.
70 Commanding Officer and Director, Navy Electronics Laboratory, San Diego 52, Calif.
71 Commanding Officer, U.S. Naval Mine Defense Lab., Panama City, Fla.
72- 73 Commanding Officer, U.S. Naval Radiological Defense Laboratory, San Francisco, Calif. ATTN: Tech. Info. Div.
74- 76 Officer-in-Charge, U.S. Naval Civil Engineering R&E Lab., U.S. Naval Construction Bn. Center, Port Hueneme, Calif. ATTN: Code 753
77 Commanding Officer, U.S. Naval Schools Command, U.S. Naval Station, Treasure Island, San Francisco, Calif.
78 Superintendent, U.S. Naval Postgraduate School, Monterey, Calif.
79 Commanding Officer, U.S. Fleet Sonar School, U.S. Naval Base, Key West, Fla.
80 Commanding Officer, U.S. Fleet Sonar School, San Diego 47, Calif.
81 Officer-in-Charge, U.S. Naval School, CEC Officers, U.S. Naval Construction Bn. Center, Port Hueneme, Calif.
82 Commanding Officer, Nuclear Weapons Training Center, Atlantic, U.S. Naval Base, Norfolk 11, Va. ATTN: Nuclear Warfare Dept.
83 Commanding Officer, Nuclear Weapons Training Center, Pacific, Naval Station, San Diego, Calif.
84 Commanding Officer, U.S. Naval Damage Control Tng. Center, Naval Base, Philadelphia 12, Pa. ATTN: ABC Defense Course
85 Commanding Officer, Air Development Squadron 5, VX-5, China Lake, Calif.

[redacted]

86 Director, Naval Air Experiment Station, Air Material Center, U.S. Naval Base, Philadelphia, Pa.
87 Commander, Officer U.S. Naval Air Development Center, Johnsville, Pa. ATTN: NAS, Librarian
88 Commanding Officer, U.S. Naval Medical Research Institute, National Naval Medical Center, Bethesda, Md.
89- 90 Commanding Officer and Director, David W. Taylor Model Basin, Washington 7, D.C. ATTN: Library
91 Commanding Officer and Director, U.S. Naval Engineering Experiment Station, Annapolis, Md.
92 Commander, Norfolk Naval Shipyard, Portsmouth, Va. ATTN: Underwater Explosions Research Division
93- 96 Commandant, U.S. Marine Corps, Washington 25, D.C. ATTN: Code A03H
97 Commandant, U.S. Coast Guard, 1300 E. St., NW, Washington 25, D.C. ATTN: (OIN)
98 Commanding Officer, U.S. Naval CIC School, U.S. Naval Air Station, Glynco, Brunswick, Ga.

AIR FORCE ACTIVITIES

99 Assistant for Atomic Energy, HQ, USAF, Washington 25, D.C. ATTN: DCS/O
100 Deputy Chief of Staff, Operations HQ. USAF, Washington 25, D.C. ATTN: Operations Analysis
101 Director of Civil Engineering, HQ. USAF, Washington 25, D.C. ATTN: AFOCE
102-103 Assistant Chief of Staff, Intelligence, HQ. USAF, Washington 25, D.C. ATTN: AFCIN-3B
104 Director of Research and Development, DCS/D, HQ. USAF, Washington 25, D.C. ATTN: Guidance and Weapons Div.
105 The Surgeon General, HQ. USAF, Washington 25, D.C. ATTN: Bio.-Def. Pre. Med. Division
106 Commander-in-Chief, Strategic Air Command, Offutt AFB, Neb. ATTN: OAWS
107 Commander, Tactical Air Command, Langley AFB, Va. ATTN: Doc. Security Branch
108 Commander, Air Defense Command, Ent AFB, Colorado. ATTN: Atomic Energy Div., ADLAN-A
109 Commander, Air Force Ballistic Missile Div. HQ. ARDC, Air Force Unit Post Office, Los Angeles 45, Calif. ATTN; WDSOT
110 Commander, Hq. Air Research and Development Command, Andrews AFB, Washington 25, D.C. ATTN: RDRWA
111-112 Commander, AF Cambridge Research Center, L. G. Hanscom Field, Bedford, Mass. ATTN: CRQST-2
113-117 Commander, Air Force Special Weapons Center, Kirtland AFB, Albuquerque, N. Mex. ATTN: Tech. Info. & Intel. Div.
118-119 Director, Air University Library, Maxwell AFB, Ala.
120 Commander, Lowry AFB, Denver, Colorado. ATTN: Dept. of Sp. Wpns. Tng.
121 Commandant, School of Aviation Medicine, USAF, Randolph AFB, Tex. ATTN: Research Secretariat
122 Commander, 1009th Sp. Wpns. Squadron, HQ. USAF, Washington 25, D.C.
123-125 Commander, Wright Air Development Center, Wright-Patterson AFB, Dayton, Ohio. ATTN: WCOSI
126-127 Director, USAF Project RAND, VIA: USAF Liaison Office, The RAND Corp., 1700 Main St., Santa Monica, Calif.
128 Commander, Rome Air Development Center, ARDC, Griffiss AFB, N.Y. ATTN: The Documents Library, RCSSLD
129 Commander, Air Technical Intelligence Center, USAF, Wright-Patterson AFB, Ohio. ATTN: AFCIN-4Bla, Library
130 Assistant Chief of Staff, Intelligence, HQ. USAFE, APO 633, New York, N.Y. ATTN: Directorate of Air Targets
131 Commander-in-Chief, Pacific Air Forces, APO 953, San Francisco, Calif. ATTN: PFCIE-MB, Base Recovery

OTHER DEPARTMENT OF DEFENSE ACTIVITIES

132 Director of Defense Research and Engineering, Washington 25, D.C. ATTN: Tech. Library
133 Chairman, Armed Services Explosives Safety Board, DOD, Building T-7, Gravelly Point, Washington 25, D.C.
134 Director, Weapons Systems Evaluation Group, Room 1E880, The Pentagon, Washington 25, D.C.
135-144 Chief, Defense Atomic Support Agency, Washington 25, D.C.
145 Commander, Field Command, DASA, Sandia Base, Albuquerque, N. Mex.
146 Commander, Field Command, DASA, Sandia Base, Albuquerque, N. Mex. ATTN: FCTG
147-151 Commander, Field Command, DASA, Sandia Base, Albuquerque, N. Mex. ATTN: FCWT
152 Commander, JTF-7, Arlington Hall Station, Arlington 12, Va.
153 Administrator, National Aeronautics and Space Administration, 1520 "H" St., N.W., Washington 25, D.C. ATTN: Mr. R. V. Rhode
154 U.S. Documents Officer, Office of the United States National Military Representative - SHAPE, APO 55, New York, N.Y.

ATOMIC ENERGY COMMISSION ACTIVITIES

155-157 U.S. Atomic Energy Commission, Technical Library, Washington 25, D.C. ATTN: For IMA
158-159 Los Alamos Scientific Laboratory, Report Library, P.O. Box 1663, Los Alamos, N. Mex. ATTN: Helen Redman
160-164 Sandia Corporation, Classified Document Division, Sandia Base, Albuquerque, N. Mex. ATTN: H. J. Smyth, Jr.
165-167 University of California Lawrence Radiation Laboratory, P.O. Box 808, Livermore, Calif. ATTN: Clovis G. Craig
168 Essential Operating Records, Div. of Infor. Services for Storage at ERC-H. ATTN: John E. Hans, Chief, Headquarters Records and Mail Service Branch, U.S. AEC, Washington 25, D.C.
169 Weapon Data Section, Technical Information Service Extension, Oak Ridge, Tenn.
170-200 Technical Information Service Extension, Oak Ridge, Tenn. (Surplus)

[redacted]

UNCLASSIFIED

[redacted]

[redacted]

[redacted]

UNCLASSIFIED